Fachbereich Physik und Fachbereich Biologie/Chemie der Universität Osnabrück[1])

Characterization of Photorefractive LiNbO₃ Waveguides Fabricated by Combined Proton and Copper Exchange

By

F. Rickermann, D. Kip, B. Gather, and E. Krätzig

Photorefractive planar waveguides in LiNbO₃ are fabricated by a combined proton and copper exchange. The dependence of refractive index profiles, optical absorption, and electrooptic coefficients on different fabrication steps is investigated. With holographic methods dark and photoconductivity, holographic sensitivity, and light-induced refractive index change in the waveguides are measured. By the additional copper exchange the steady state diffraction efficiency of holographic gratings in our proton-exchanged waveguides is increased from 0.01 to 65%.

1. Introduction

LiNbO₃ is a promising material for holographic volume storage and integrated optics because of its electrooptical, elastooptical, and piezoelectric properties [1]. In contrast to bulk samples it is easy to obtain high light intensities with moderate input powers in waveguides; large photorefractive effects are observed. Therefore photorefractive waveguides may be used as integrated optical switches, sensors, or memory cells [2, 3].

Fabrication of waveguides in LiNbO₃ often requires some technological efforts, for example high-temperature diffusion ($\approx 1000\ ^\circ\text{C}$) of transition metals [4] or ion implantation [5]. A simpler technique to produce waveguides is proton exchange in benzoic acid taking place already at rather low exchange temperatures ($\approx 250\ ^\circ\text{C}$) and yielding high extraordinary refractive index changes [6].

An undesired feature of proton-exchanged LiNbO₃ waveguides produced in pure benzoic acid, however, is the degradation of electrooptic coefficients [7]. This degradation may be partially avoided by the use of buffered benzoic acid or by annealing treatments after the proton exchange process [8].

To utilize photorefractive properties of the waveguides enhancement of light-induced refractive index changes is of particular importance. This may be realized by additional ion exchange (Fe^{2+}, Cu^+). First results on doping of proton-exchanged waveguides with copper were published by Kostritskii and Kolesnikov [9]. This extra technological step may also be performed at rather low temperatures.

In this paper we report on investigations of this combined proton and copper exchange technique in LiNbO₃. The dependence of the waveguide properties on different fabrication steps is analyzed. We determine refractive index profiles, copper profiles, optical absorption,

---

[1]) Barbarastr. 7, D-49069 Osnabrück, Federal Republic of Germany.

and electrooptic coefficients. Finally, the waveguides are used to record holographic gratings. Dark and photoconductivity, holographic sensitivity, and light-induced refractive index change in the waveguides are investigated.

2. Experimental Methods

For the preparation of the waveguides we use polished x- and z-cut $LiNbO_3$ substrates of congruently melting composition. The preparation is divided into four steps. At first proton-exchanged $LiNbO_3$ waveguides are formed by immersing the substrates into molten benzoic acid (C_6H_5COOH) at a fixed temperature of 250 °C. To prevent surface damage, C_6H_5COOLi (1 mol%) is added to the benzoic acid for lithium buffering. The exchange time ranges from 1 to 8 h for different samples. In a second step we dope the proton-exchanged waveguides with copper by immersing them into molten benzoic acid mixed with 1 to 11 mol% Cu_2O at a temperature of 250 °C for 10 to 60 min. Then the waveguides are oxidized in $LiNO_3$ at a temperature of 250 °C varying the oxidation time from 10 to 60 min. Finally we anneal the waveguides at a temperature of 400 °C for 10 min to 6 h. The fabrication parameters for the different samples are summarized in Table 1.

The effective refractive indices n_{eff} of TE and TM modes are measured with the help of the prism coupling method (dark line spectroscopy) [10]. The coupling angles φ_{eff} are detected and converted into effective refractive indices,

$$n_{eff} = n_p \left(\alpha + \arcsin \left(\frac{n_{air}}{n_p} \sin \varphi_{eff} \right) \right),$$

where n_p is the refractive index of the used rutile prism, n_{air} the refractive index of air, and α the relevant prism angle. From the effective refractive indices the profiles of ordinary and extraordinary refractive index are reconstructed by the use of an inverse WKB method [11].

The copper concentration profile is measured with an electron microprobe (acceleration voltage 25 keV, beam width 0.2 µm, step width 0.3 µm). We polish one face of the substrate

Table 1
Waveguide notation, cut direction, and fabrication parameters for all investigated samples

waveguide		fabrication		
notation	cut	time [min]	temp. [°C]	process
H1	x	120	250	BA
H2	z	30	250	BA
		340	400	air
HCu1 to 5	x	120	250	BA
HCu1 to 3		10	250	BA + 3, 7, 11 mol% Cu_2O
HCu4, 5		30, 60	250	BA + 3 mol% Cu_2O
HCu6	z	480	250	BA + 1 mol% LB
		30	250	BA + 1 mol% Cu_2O
		20	250	$LiNO_3$
		190	400	air
		13 + 10	250	$LiNO_3$

BA denotes benzoic acid and LB lithiumbenzoat

perpendicular to the waveguiding layer. The electron beam scans this polished face starting from the top of the waveguiding layer. To get absolute values of the copper concentration at the surface of the waveguides, X-ray photoelectron spectroscopy (XPS) is employed.

The electrooptic coefficient of the waveguides is determined by the method of attenuated total reflection [12]. For the measurement two gold electrodes (electrode width 1.5 mm, electrode distance 2 mm) are vacuum-deposited on the surface of the waveguiding layer. By applying an alternating voltage of ± 1000 V between the two electrodes the refractive index of the waveguide is modulated via the electrooptic effect. Thus the angle φ_{eff} of the reflectivity minima of the dark line spectrum is modulated. This leads to a modulation ΔR of reflected intensity in the dark line spectrum for constant angle φ_{eff} which is detected by a lock-in amplifier and can be related to the electrooptical coefficient,

$$r_{333} = \frac{2}{n_{\mathrm{eff}}^3} \frac{\Delta R}{\partial R/\partial \varphi} \frac{1}{\partial \varphi_{\mathrm{eff}}/\partial n_3} \frac{1}{\Delta E}.$$

Here ΔE is the peak-to-peak electric field amplitude. In this way it is only possible to measure the electrooptic coefficient r_{333}, because in proton-exchanged x-cut LiNbO$_3$ waveguides only light polarized parallel to the crystal c-axis is guided.

To investigate dark and photoconductivity, holographic sensitivity, and light-induced refractive index change, holographic gratings are written and erased in planar z-cut LiNbO$_3$ waveguides utilizing an argon-ion laser (wavelength 514.5 nm). For this purpose two beams are coupled into and out of the waveguide using rutile prisms. Depending on the angle the light enters the prism, and different extraordinarily (TM) polarized modes are excited. Because the refractive index profiles of the investigated waveguides have a nearly Gaussian form, we are able to perform measurements in dependence of the depth of excited modes. The depth z_{M} of a mode is defined as center of intensity $|E_{\mathrm{M}}|^2$,

$$z_{\mathrm{M}} = \int |E_{\mathrm{M}}(z)|^2 \, z \, \mathrm{d}z / \int |E_{\mathrm{M}}(z)|^2 \, \mathrm{d}z \, .$$

In the experimental setup (Fig. 1) two modes intersect at an angle of $2\theta = 4.4°$ (grating period 3 µm) and the interaction length in the waveguide is $l = 2.5$ mm (beam diameter 0.4 mm). During build-up of a refractive index grating, the diffraction efficiency is measured as a function of time by blocking one of the beams for a short moment (50 ms) and measuring the ratio of diffracted and total light intensity of the outcoupled beams. When the saturation value of diffraction efficiency is reached, one of the beams is switched off, and the diffracted light intensity indicates the decay of the grating during readout. The relation between diffraction efficiency and refractive index change is given by Kogelnik's formula [13],
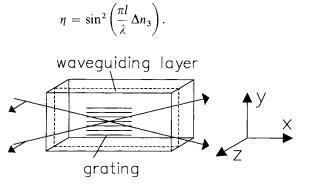
$$\eta = \sin^2\left(\frac{\pi l}{\lambda} \Delta n_3\right).$$

Fig. 1. Configuration for writing holographic gratings in z-cut LiNbO$_3$ waveguides using extraordinarily polarized light (schematic). The propagation directions and polarizations of the interacting waves are indicated by arrows

Recording and erasure of holographic gratings are well described by exponential relations
[14, 15],

recording: $\Delta n_e(t) = \Delta n_e^s (1 - e^{-t/\tau})$,

erasure: $\Delta n_e(t) = \Delta n_e^s \, e^{-t/\tau}$,

where Δn_e^s denotes the saturation value of ligh-induced refractive index change and t the
time of writing and erasure, respectively. From the time constant τ of erasure we deduce
the conductivity $\sigma_{33} = \varepsilon_{33}^{st}\varepsilon_0/\tau$ ($\varepsilon_{33}^{st} = 32$ [1]). The holographic sensitivity is defined by

$$S = \frac{d(\Delta n)}{d(I_{tot}t)}\bigg|_{t=0},$$

where I_{tot} is the entire intensity in the waveguide.

3. Waveguide Properties and Fabrication Steps

We analyze the dependence of the waveguide properties on the four fabrication steps: proton
exchange, copper doping, oxidation, and annealing. Furthermore, we report on surface
damage and stress-induced grating-like structures in the waveguides.

3.1 Proton exchange

After the treatment of an x-cut LiNbO$_3$ substrate in pure benzoic acid for 2 h we are able
to excite TE modes and weak TM modes. Using mode spectroscopy and an inverse WKB
method we reconstruct the profiles of ordinary and extraordinary refractive index of the
waveguide H1. Results are shown in Fig. 2. To get a complete ordinary refractive index
profile we use as lowest reconstructed ordinary refractive index the substrate value of
LiNbO$_3$ ($n_0 = 2.33$). Both profiles, ordinary and extraordinary, are step-like with a thickness
of $d = (3.2 \pm 0.2)$ μm. The extraordinary refractive index is increased ($\Delta n_e \approx 0.16$), while
the ordinary refractive index is decreased ($\Delta n_0 \approx -0.05$). Qualitatively, the ordinary
refractive index profile shows a barrier resulting from a LiNb$_3$O$_8$ phase at the proton
diffusion front with a lower refractive index than LiNbO$_3$ [16]. The high optical absorption
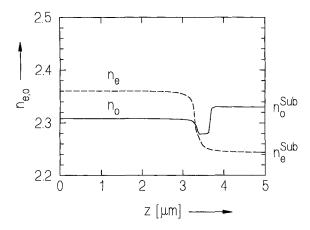

Fig. 2. Ordinary and extraordinary refractive indices n_e and n_0 vs. depth z (waveguide H1)

$(\alpha > 2\ \text{mm}^{-1})$ measured for the weak TM modes points to substrate modes resulting from the low width and depth of the ordinary refractive index barrier. The absorption coefficient of the TE modes is about $\alpha = 0.1\ \text{mm}^{-1}$.

3.2 Copper doping

To increase the photorefractive sensitivity, the waveguides are additionally doped with copper. Fig. 3 illustrates the copper concentration c_{Cu}, measured with an electron micro-probe, for the set of waveguides HCu1 to HCu5. The copper concentration profiles have a nearly Gaussian form. Larger copper concentrations in the benzoic acid melt and longer exchange times lead to higher copper concentration and exchange depth in the waveguide. In comparison to the waveguide thickness of $d = 2.9\ \mu\text{m}$ the maximum copper exchange depth ($\approx 1.0\ \mu\text{m}$) is relatively small. The diffusion constant of Cu in proton-exchanged LiNbO₃ waveguides after a treatment in benzoic acid melt with 3 mol% copper is evaluated as $D_{Cu} = 0.15\ \mu\text{m}^2/\text{h}$. But it should be mentioned that the diffusion constant of Cu mainly depends on the parameters of previous proton exchange. Using X-ray photoelectron spectroscopy, we determine a copper concentration of (0.5 ± 0.1) mol% at the surface of the waveguide HCu2.

3.3 Oxidation treatment

A high optical absorption between 380 and 500 nm appears in the waveguide after copper exchange. This is attributed to the appearance of Cu^+ centers [17]. The absorption constant can be estimated as $\alpha > 2\ \text{mm}^{-1}$. Because of this relatively high absorption it is not possible to perform holographic measurements in the waveguides before decreasing the Cu^+ concentration by oxidation of these centers to Cu^{2+}. In Fig. 4 the optical absorption coefficients α in the waveguiding layer for different depths are shown as a function of oxidation time. The optical absorption coefficient decreases with increasing waveguide
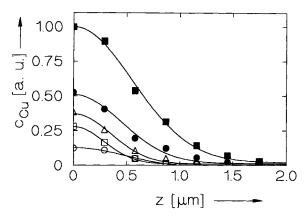
Fig. 3. Copper concentration (arbitrary units) measured with an electron microprobe as a function of the waveguide depth z for the set of waveguides HCu1 to HCu5. Here the exchange time and the copper concentration in the benzoic acid are varied. The thickness of these waveguides is $d = 2.9\ \mu\text{m}$. ○: HCu1, 10 min BA + 3 mol% Cu₂O; □: HCu2, 10 min BA + 7 mol% Cu₂O; △: HCu3, 10 min BA + 11 mol% Cu₂O; ●: HCu4, 30 min BA + 3 mol% Cu₂O; ■: HCu5, 60 min BA + 3 mol% Cu₂O (abbreviations see Table 1)
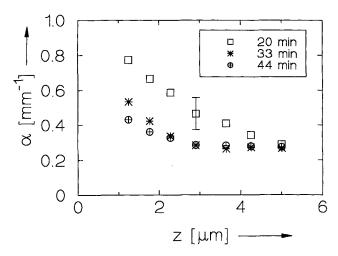
Fig. 4. Optical absorption coefficient α vs. waveguide depth z for different oxidation times in $LiNO_3$ at $T = 250\,°C$ for the waveguide HCu6

depth. This is caused by a larger copper concentration near the surface of the waveguide. For larger oxidation times α is reduced for all modes because of the change of the $c_{Cu^+}/c_{Cu^{2+}}$ ratio to lower values. In this way it is possible to decrease α again to about 0.4 mm^{-1} for the TM_0 mode.

3.4 Annealing

It is well known that in proton-exchanged $LiNbO_3$ waveguides electrooptic coefficients are reduced [7]. Annealing treatments again enhance the electrooptic coefficients to nearly the $LiNbO_3$ values, but these treatments also change the index profile from step-like to Gaussian form [20]. Furthermore, deformations and strains, mode diffraction and optical loss in the waveguiding layer are lowered [18]. With the attenuated total reflection method [12] we determine the electrooptic coefficient r_{333} for different TE modes in the x-cut proton-exchanged waveguide H2 as a function of extraordinary refractive index change (Fig. 5). The waveguide is successively annealed (time interval 20 min) and then the coefficient r_{333} is measured. For $\Delta n_e = 0.03$ to 0.09, r_{333} is lowered from 30 pmV^{-1} to zero. This behavior may be explained by taking into account structural changes of rhombohedral, monoclinic, and cubic phases with various proton concentrations x in the $Li_{1-x}H_xNbO_3$ system. The waveguiding layer has a cubic structure for a high proton concentration ($0.77 < x < 1$) [21]. In this phase no linear electrooptic coefficients exist, confirmed by our experiment. Annealing the waveguide H2 at a temperature of 400 °C for 320 min, leads to an extraordinary refractive index change $\Delta n_e < 0.03$. As shown in Fig. 5, in this range of Δn_e the electrooptic coefficient is approximately $r_{333} = 30$ pmV^{-1}. This fairly well agrees with the value of r_{333} for $LiNbO_3$ [1]. By annealing the waveguide, we change the crystal structure to the rhombohedral phase. Thus the coefficient r_{333} is increased and reaches again the value of the substrate.

Large electrooptic coefficients are of advantage for holographic measurements. As can be seen from Fig. 5, Δn_e has to be smaller than 0.03 to optimize r_{333} in the waveguide. In proton- and copper-exchanged x-cut waveguides we obtain the same results.
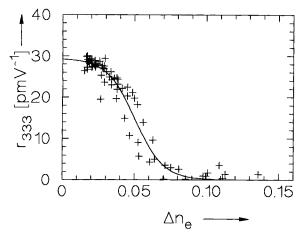
Fig. 5. Electrooptic coefficient r_{333} vs. extraordinary refractive index change Δn_e for the proton-exchanged waveguide H2

3.5 Surface damage

With the investigation of proton exchange in x-cut and z-cut LiNbO$_3$ we observe cracks in the substrate surfaces for long exchange and oxidation times. This surface damage is caused by the change of crystal structure (Li$_{1-x}$H$_x$NbO$_3$ with $0 < x < 1$) in the wave-guiding layer. The cracks are the results of the mismatch of lattice constants between a strongly proton-exchanged region near the surface of the waveguide and regions deeper in the waveguide where less exchange has taken place [18]. Samples with cracks cannot be used for further optical investigations because of strong light scattering in the wave-guiding layer. In x-cut substrates cracks arise at the surface after treatments in pure benzoic acid for $t > 190$ min, while in z-cut substrates no cracks are detected after $t = 46$ h. Copper exchange does not create additional cracks. But even in the case of a low copper concentration in x-cut and z-cut waveguiding layers (< 50 min in benzoic acid $+ 1$ mol% Cu$_2$O) surface cracks often appear after oxidation at a temperature of 250 °C for several minutes.

In strongly proton- and copper-doped waveguides the light of an excited mode is diffracted into other modes. Furthermore, the mode spectrum is anomalously side-shifted out of the expected geometrical plane. This effect can be explained assuming the existence of precisely oriented, stress-induced grating-like structures with irregular periods in the waveguides [19]. The stress-induced structures result from the mismatch of lattice constants described above. In x-cut LiNbO$_3$ this effect appears after proton exchange, in z-cut substrates only after copper exchange.

Thus we use z-cut LiNbO$_3$ for the fabrication of photorefractive waveguides because grating-like structures and substrate damage are less pronounced in comparison to x-cut LiNbO$_3$. However, only a small range of parameters is allowed to fabricate good photorefractive waveguides. The technology is further modified to largely avoid surface damage. Proton- and copper-exchanged waveguides are oxidized at first for a few minutes, then they are annealed, and finally oxidized again. In Table 1 the parameters for fabricating the photorefractive waveguides HC6 are also included.
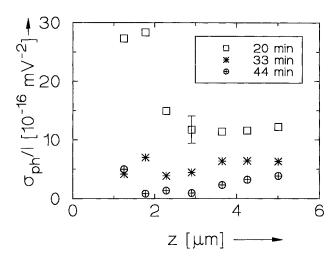
Fig. 6. Specific photoconductivity σ_{ph}/I vs. waveguide depth z for different oxidation times in LiNO$_3$ at $T = 250\,°C$ (waveguide HCu6)

4. Holographic Characterization

We use holographic methods to investigate dark and photoconductivity, holographic sensitivity, and light-induced refractive index change in the waveguide for different oxidation states. Holographic gratings are written in the z-cut LiNbO$_3$ waveguides HCu6 with two extraordinarily (TM) polarized modes. To reduce m-line scattering an input power of 200 µW for each mode is used. Writing of a holographic grating in copper- and proton-exchanged waveguides leads to a steady state diffraction efficiency of 65% after one minute corresponding to a light-induced refractive index change of 3×10^{-3}. Without additional copper exchange we only obtain 0.01% ($\Delta n_e^s \leq 2 \times 10^{-5}$).

In the geometry used here, photovoltaic currents in the direction normal to the waveguide surface are excited, while the grating vector in the waveguiding layer is nearly perpendicular to the propagation direction. Decisive for the formation of a grating is the small thickness of the waveguiding layer, which is comparable to the grating period [22].
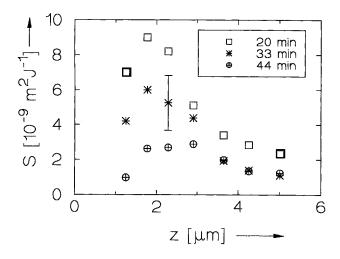

Fig. 7. Holographic sensitivity S vs. waveguide depth z for different oxidation times in LiNO$_3$ at $T = 250\,°C$ (waveguide HCu6)
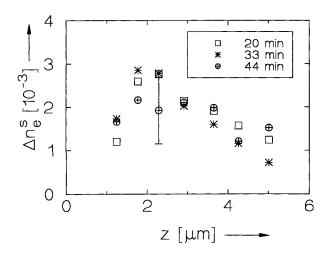
Fig. 8. Saturation value of light-induced refractive index change Δn_e^s vs. waveguide depth z for different oxidization times in LiNO$_3$ at $T = 250\ ^\circ$C (waveguide HCu6)

For the TM$_0$ mode we measure a dark conductivity σ_d of $5 \times 10^{-12}\ \Omega^{-1}\ m^{-1}$. The holographic gratings are erased in the dark within a few minutes. In comparison to the substrate value the dark conductivity in proton-exchanged waveguides is increased by about three orders of magnitude.

As can be seen in Fig. 6 and 7 the specific photoconductivity and the holographic sensitivity decrease, if the $c_{Cu^+}/c_{Cu^{2+}}$ ratio is diminished by oxidation. These results agree with the relations $\sigma_{ph}/I \sim c_{Cu^+}/c_{Cu^{2+}}$ and $S \sim c_{Cu^+}$ derived for LiNbO$_3$:Cu crystals [23]. The model is supported which assumes Cu$^+$ ions to act as filled and Cu^{2+} ions as empty traps [17]. The values of specific photoconductivity range from (1 to 30) $\times 10^{-16}$ mV^{-2}. For the used intensities the photoconductivity is one order of magnitude larger than the dark conductivity. The holographic sensitivity ranges from (1 to 9) $\times 10^{-9}\ m^2\ J^{-1}$. For the saturation value of light-induced refractive index change we cannot observe a dependence on the oxidation state of the waveguide. This may be caused by a considerable scattering of the measured values which range from 0.8×10^{-3} to 3×10^{-3} (Fig. 8).

We also observe a decrease of dark conductivity, specific photoconductivity, holographic sensitivity, and saturation value of light-induced refractive index change with increasing waveguide depth. This may be explained with a decreasing overlap of the intensity distribution of higher modes with the depth profile of copper. In addition, the low values of these parameters for the TM$_0$ mode may result from strong m-line scattering for this mode.

5. Conclusions

By an additional copper exchange the photorefractive properties of proton-exchanged LiNbO$_3$ waveguides are considerably improved. We succeeded in increasing the holographic steady state diffraction efficiency to 65%, corresponding to an increase of light-induced refractive index change Δn_e^s to 3×10^{-3}. Four fabrication steps are necessary: proton exchange, copper doping, oxidation, and annealing. Best results are obtained with z-cut substrates. The processes may be performed at moderate temperatures ($\approx 250\ ^\circ$C). Annealing treatments at temperatures of 400 $^\circ$C are necessary in any case to get sufficiently large electrooptic coefficients in the waveguides. Optical absorption may be controlled by

oxidation processes, then values of about 0.4 mm^{-1} are measured. The method is also of interest for $LiTaO_3$ crystals. Here the Curie temperature is about 620 °C and indiffusion processes at high temperatures require additional poling.

References

[1] R. S. Weis and T. K. Gaylord, Appl. Phys. A **37**, 191 (1985).
[2] V. E. Wood, P. J. Cressman, R. L. Holman, and C. M. Verber, in: Photorefractive Materials and Their Applications II, Topics appl. Phys., Vol. **61**, Ed. P. Günter and J.-P. Huignard, Springer-Verlag, 1989 (pp. 45 to 100).
[3] A. Donaldson, J. Phys. D **24**, 785 (1991).
[4] R. V. Schmidt and I. P. Kaminov, Appl. Phys. Letters **25**, 458 (1974).
[5] K. Wenzlik, J. Heibei, and E. Voges, phys. stat. sol. (a) **61**, K207 (1980).
[6] V. A. Ganshin and Yu. N. Korkishko, phys. stat. sol. (a) **119**, 11 (1990).
[7] P. G. Suchoski, T. K. Findakly, and F. J. Leonberger, Optics Letters **13**, 1050 (1988).
[8] M. Rottschalk, A. Rasch, and W. Karthe, Optics Commun. **10**, 138 (1989).
[9] S. M. Kostritskii and O. M. Kolesnikov, J. Opt. Soc. Amer. **B11**, 1674 (1994).
[10] P. K. Tien, R. Ulrich, and R. J. Martin, Appl. Phys. Letters **14**, 291 (1969).
[11] P. Hertel and H. P. Menzler, Appl. Phys. B **44**, 75 (1987).
[12] V. Dentan, Y. Lévy, M. Dumont, P. Robin, and E. Chastaing, Optics Commun. **69**, 379 (1989).
[13] H. Kogelnik, Bell Syst. tech. J. **48**, 2909 (1969).
[14] N. V. Kukhtarev, V. B. Markov, S. G. Odoulov, M. S. Soskin, and V. L. Vinetskii, Ferroelectrics **22**, 949 (1979).
[15] E. Krätzig, Ferroelectrics **104**, 257 (1990).
[16] V. A. Ganshin, V. Sh. Ivanov, Yu. N. Korkishko, and V. Z. Petrova, Soviet Phys. – Tech. Phys. **31**, 794 (1986).
[17] E. Krätzig and R. Orlowski, Ferroelectrics **27**, 241 (1980).
[18] M. Minakata, K. Kumagai, and S. Kawakami, Appl. Phys. Letters **49**, 992 (1986).
[19] M. De Micheli and P. St. J. Russel, Appl. Optics **25**, 3896 (1986).
[20] V. A. Ganshin and Yu. N. Korkishko, Optics Commun. **86**, 523 (1991).
[21] C. E. Rice and J. L. Jackel, Mater. Res. Bull. **19**, 591 (1984).
[22] D. Kip, F. Rickermann, and E. Krätzig, Optic Letters **20**, 1139 (1995).
[23] R. Sommerfeld, R. A. Rupp, H. Vormann, and E. Krätzig, phys. stat. sol. (a) **99**, K15 (1987).